

Tunable Wet Adhesion of Sprayable Microgel Glues Driven by a Phase Transition in Polymer Networks

Ting Zhao, Haojie Zhang, Jinmeng Zhang, Wen Chen, Jianda Xie, and Weitai Wu*



Cite This: ACS Macro Lett. 2025, 14, 671–678



Read Online

ACCESS |

Metrics & More

Article Recommendations

Supporting Information

ABSTRACT: With the emergence of human-computer interaction and related fields, how to realize tunable adhesion on wet and soft materials has become an important issue. In this letter, we propose a strategy for tunable wet adhesion by leveraging the phase transition of polymeric nanoparticles to achieve dynamic, multiscale, and multifactorial synergistic modulation. The strategy is validated by using stimuli-responsive polymer microgel dispersions as sprayable glues, which can switch between swollen and deswollen states through phase transitions, thereby tuning interfacial water molecules. This process dynamically tunes microscopic molecular interactions and the mesoscopic contact area between microgel nanoparticles and the substrate surface, as well as the cohesion within interfacial microgel layers. As a result, adhesion is enhanced in the swollen state, reaching about 373 N m^{-1} , while it is weakened in the deswollen state due to water release. The tunable wet adhesion is reproducible, making the sprayable microgel glues of potential interest for applications (e.g., in hydrogel-based sensors for human motion detection).



Wet adhesives play a crucial role in various fields and are extensively utilized in human-computer interaction,¹ wearable sensors,² soft robot,³ tissue repair,⁴ and drug delivery.⁵ However, the presence of an interfacial hydration layer prevents direct contact between the adhesive and the substrate, resulting in weak adhesion.⁶ Existing research primarily focuses on achieving strong interfacial adhesion by removing interfacial moisture. However, in practical applications, adhesives must not only maintain strong adhesion to the substrate but also offer adjustable detachment capabilities. For instance, epidermal wearable devices require long-term wear and frequent replacement. Without adjustable adhesion properties, such devices may cause skin damage.^{8,9} Therefore, the development of smart adhesives with tunable adhesion, which can maintain strong adhesion in humid environments while switching to weak adhesion for detachment under controlled conditions, has become a major challenge in modern bonding technologies.¹⁰

Currently, the development of smart switchable adhesives is primarily focused on solid-like adhesives (such as tapes or gels). While these solid adhesives can partially remove interfacial water to enhance wet adhesion, their limited ability to fill molecular microcavities on the substrate surface results in weaker adhesion.^{11,12} When switching adhesion, macroscopic solid-like gel may reduce adhesion switching efficiency due to a large number of underutilized contact zones (microcavities on the surface).^{11,13} On the other hand, solid-like adhesives cannot be manipulated arbitrarily due to self-adhesion.^{14,15} In nature, animals such as geckos, tree frogs, and certain insects

have evolved strategies that enable them to reversibly adhere to nearly any surface. This is achieved through contact-splitting adhesion between the micronano structures on their feet and contact surfaces, relying on van der Waals and/or capillary forces.^{16–19} As a result, nanoparticle dispersions have been explored as adhesives, demonstrating their ability to serve as interfacial connectors that bind hydrogels or biological tissues together.^{14,20,21} Moreover, nanoparticle dispersions can be easily and flexibly sprayed, coated, or diffused onto surfaces, filling microcavities on the substrate to accommodate different morphologies and thereby increasing the adhesion contact area. However, most of the nanoparticle-based adhesives developed to date rely on rigid inorganic nanoparticles, and there has been limited progress in utilizing soft, polymer-based nanoparticles in adhesive formulations.^{22,23}

In this Letter, we propose a novel strategy to achieve dynamic, multiscale, and multifactorial tunable adhesion by exploiting phase transitions in polymer networks to regulate the water content at the adhesion interface. Adhesion is an interfacial phenomenon, with nanoparticle adhesion performance influenced by factors such as surface area, morphology,

Received: March 13, 2025

Revised: May 2, 2025

Accepted: May 5, 2025

Published: May 8, 2025



and interactions with the substrate.^{24–26} Compared to rigid nanoparticles, soft polymer microgel nanoparticles offer enhanced surface functionalization, rapid responsiveness, and superior interfacial adaptability.^{27–29} Inspired by the strong adhesive properties of the micronano structures on gecko toes, microgels can be easily engineered to replicate similar structures.^{17,30} This makes it an ideal material for achieving tunable adhesion in wet and soft environments. Based on these characteristics, as a proof-of-concept, we designed a thermoresponsive, tunable microgel incorporating guanidinium cation as glue. The glue regulates the water content at the adhesion interface through the polymer's phase transition, thus modulating the noncovalent interactions and the contact area between guanidinium cation and the adhesive substrate, and the cohesion within the interfacial microgel layer, enabling control over adhesion. The adhesives can be applied to hydrogel strain sensors for detecting human motion.

The microgels (denoted as PGE) were synthesized in water (150.0 mL) via free radical polymerization of 2-(2-methoxyethoxy)ethyl methacrylate (MEO₂MA; 2.25×10^{-2} mol) and N-(3-methacrylamidopropyl) guanidinium chloride (GPMA; 5.625×10^{-3} mol, Figure S1), in the presence of ethylene glycol dimethacrylate (EGDMA; 5.6×10^{-5} mol) as a cross-linker, 2,2'-azobis(2-methylpropionamidine) dihydrochloride (AAPH; 2.8×10^{-4} mol) as an initiator and hexadecyl trimethylammonium bromide (CTAB; 1.85×10^{-4} mol) under a N₂ atmosphere at 70.0 °C (Figure 1a). MEO₂MA homopolymers have a lower critical solution temperature (LCST; ca. 28.0 °C under the reaction conditions, also see below) in water,³¹ at temperatures above which they become relatively hydrophobic to allow the formation of spherical-like microgels (collected after reacting for 5 h, and then purified before characterizations). As shown in Figure S2a, the microgels exhibit a narrow size distribution in aqueous solution, along with good stability. The size distribution also remains consistent across different scattering angles (Figure S2b), suggesting that the microgels retain an approximately ideal spherical morphology in solution.³² In contrast to the wet state, the TEM and SEM images presented in Figures 1b and 1c reveal clear differences in both size distribution and morphology. These discrepancies primarily result from the fact that the samples were prepared in a dry state and imaged under high vacuum conditions. During the drying process, the microgels may undergo shrinkage, flattening, or lateral spreading on the substrate. Moreover, nonuniform interactions between the microgels and the substrate may further contribute to the observed polydispersity and deviations from ideal spherical shapes in the images.³³ In the FTIR spectrum (Figure 1d), a characteristic band of C—O—C stretching vibration (ca. 1121 cm⁻¹) for the ether oxygen groups of EGDMA unit,³⁴ and a characteristic band of O—C stretching vibration (1029 cm⁻¹) for methyl ether oxygen on MEO₂MA unit,³⁵ and that characteristic band of C=N stretching vibration (ca. 1654 cm⁻¹) for the guanidine groups of GPMA units were detected.³⁶ XPS measurement results show that N elements with binding energies of N 1s were observed around 399 eV, which can confirm the presence of guanidinium on the microgel surface (Figure 1e and Figure S3).

The microgel dispersions were evenly coated to the surface of the wet and soft substrate by spraying, followed by bringing the two substrates into contact (Figure 1a and Figure S4). Unless otherwise specified, all T-peeling tests were conducted

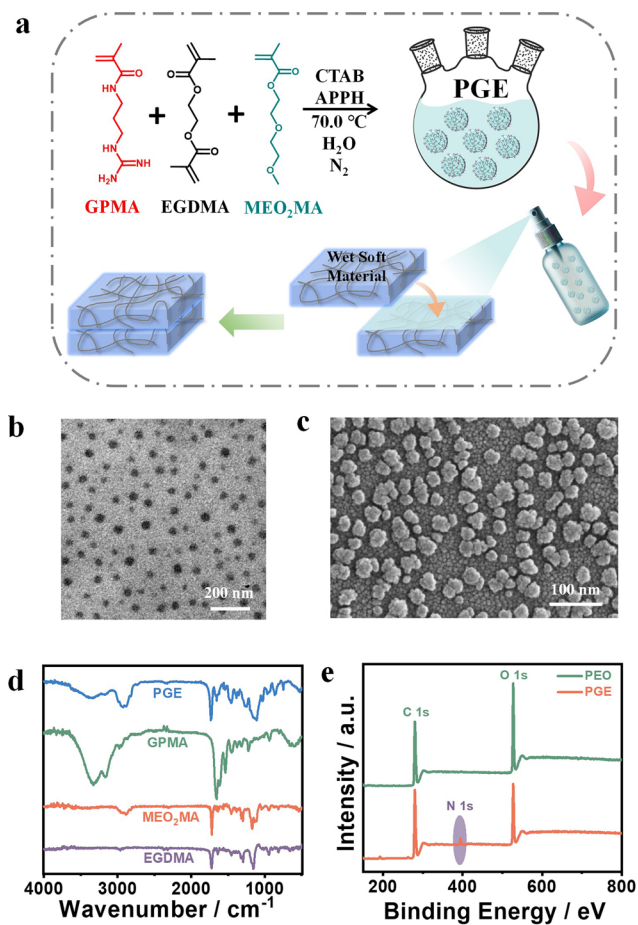


Figure 1. (a) Schematic diagram of the synthesis of PGE microgel dispersions and their adhesion to two pieces of wet and soft material by spraying. (b) Typical TEM image of the microgels. (c) Typical SEM image of the microgels. (d) A comparison of the FTIR spectra of PGE microgels, GPMA monomer, MEO₂MA monomer, and EGDMA monomer. (e) XPS spectra of the PGE and PEO microgels (PEO microgels as control samples without GPMA).

using Semi-IPN SA/PAM hydrogels as the default substrate material (Figure S5a).³⁷ In the letter, “original” refers to the adhesion between the two wet and soft substrates themselves, without the coating of the microgel dispersions. First, the concentration and volume of the microgel dispersion were optimized to achieve optimal adhesion performance. The hydrogels, which had been adhered under a compressive strain of 10% (d/L) for 24 h, were subjected to T-peeling tests (Figure S5b). As shown in Figure 2a and Figure S6, statistical significance analysis based on multiple samples revealed that the microgel dispersions exhibited the highest adhesion at a condition of 0.2 mL-2.268 wt %. This indicates that both an adequate concentration and a proper volume are essential for ensuring strong adhesion. Accordingly, 0.2 mL-2.268 wt % was selected as the adhesive conditions for all subsequent experiments. After the initial pressure treatment, the two hydrogel sheets were able to reattach directly after each T-peeling test, without the need for additional microgel dispersions or the application of external pressure. After a 5 min adhesion period, the adhesion of the hydrogels was reassessed. The adhesion efficiency was defined as the ratio of the adhesion of the readhered hydrogels to the initial adhesion. As shown in Figure 2b, under conditions without external

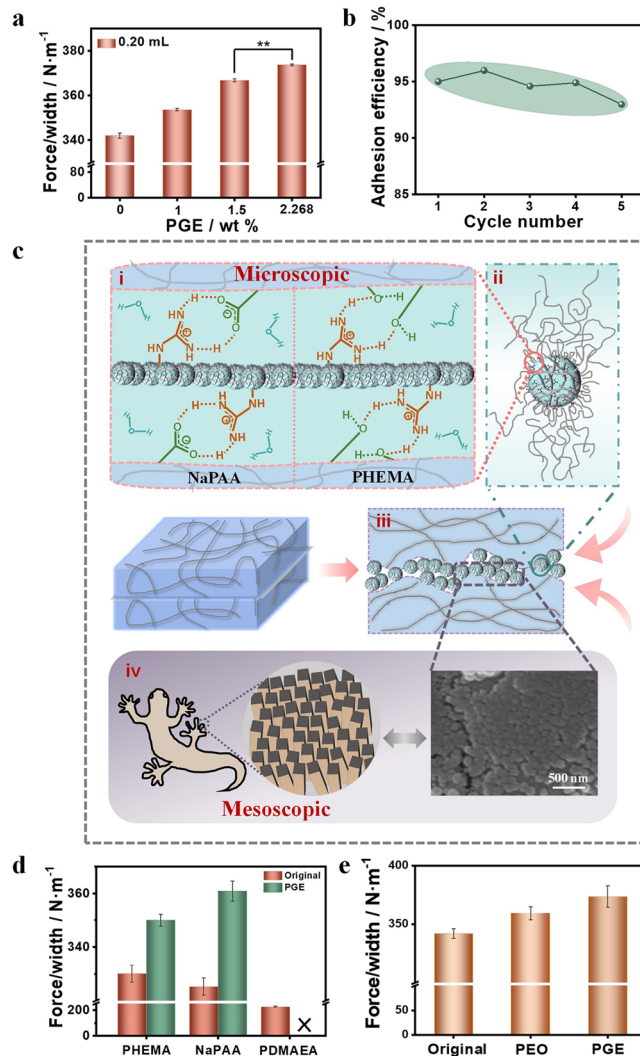


Figure 2. (a) T-peeling test results of hydrogel substrates coated with microgel dispersions at different mass fractions. The data are expressed as means \pm standard deviations of nine replicates (** $P < 0.05$). (b) Adhesion efficiency over multiple cycles under constant environmental conditions. (c) Adhesion mechanism of the microgels. (i) The primary interactions responsible for the adhesion between microgel functional groups and the substrate. (ii) The polymer chains of the substrate strongly adhere to the microgel nanoparticles through physical adsorption. (iii) The state of microgel nanoparticles between hydrogel substrates. (iv) Schematic illustration of the enlarged setae on a gecko's toe and SEM image illustrating the microgel dispersions at the adhesion interface between the hydrogel substrates. (d) T-peeling test results of the microgel dispersions coated on hydrogel substrates with different charges. X's indicate no adhesion. (e) T-peeling test of hydrogel substrates coated with different microgel dispersions. The data are expressed as means \pm standard deviations of triplicates.

stimulation, the repeatable adhesion performance of the microgel dispersion exhibits a declining trend. This decline is primarily attributed to interfacial damage accumulated during repeated use, which impairs the effective re-establishment of interfacial interactions (Figure S7).³⁸

To investigate the adhesion mechanism of microgel dispersions, a comprehensive analysis was conducted at both the microscopic molecular and mesoscopic levels (Figure 2c). At the microscopic molecular level, the adhesion properties of

GPMA incorporated within the microgels were initially investigated. T-peeling tests revealed that when the GPMA solution was applied to the hydrogel interface, its adhesion slightly exceeded that of the original hydrogel (Figure S8). This limited enhancement is attributed to the low molecular weight of GPMA, which lacks the capacity to form intermolecular covalent interactions.³⁹ Instead, the improved adhesion is likely due to the strong multivalent noncovalent interactions between guanidinium cations and the substrate,¹⁵ including bidentate hydrogen-bond-associated salt bridges with oxyanions. The planar structure of guanidinium cations also contributes to hydrophobic interactions.⁴⁰ During the adhesion process, these guanidinium cations spatially hinder the movement of water molecules, promoting dehydration of their surface, which in turn facilitates stronger interactions with the substrate. These findings underscore the significant role of the guanidino functional group in interfacial adhesion.

Furthermore, adhesion substrates were classified into neutral, negatively charged, and positively charged polymer chain groups to investigate the relationship between the interactions of different substrate components and adhesion. Hydrogel substrates with varying charges and functional groups were synthesized, including neutral Poly(hydroxyethyl methacrylate) (PHEMA), negatively charged Sodium polyacrylate (NaPAA), and positively charged 2-(Acryloyloxy)ethyl trimethylammonium chloride (PDMAEA). As shown in Figure 2d, for neutral substrate, hydrogen bonding between hydroxyl groups governs the adhesion of polymer chains to the nanoparticle surface. Compared to NaPAA alone, the microgel dispersions exhibited enhanced adhesion to NaPAA, which is attributed to the formation of multivalent salt bridges between guanidinium cations and COO⁻ groups (Figure 2c-i). The adhesion of NaPAA is higher than that of the neutral substrate due to the lack of additional electrostatic contributions.¹⁵ Conversely, PDMAEA exhibited no adhesion due to the strong electrostatic repulsion between guanidinium cations on the microgels and cationic groups on the substrate. These findings demonstrate that microgels act as connectors at the interfaces of wet and soft substrates.¹⁴ When microgels are in a swollen state, ethylene glycol and methoxy groups within the network form stable intermolecular hydrogen bonds with adjacent water molecules, creating a polymer network rich in free water. The guanidine groups on the surface of the microgels exhibit localized hydrophobic characteristics due to their planar structure, facilitating the formation of hydrogen bonds or multivalent salt-bridge interactions.⁴⁰ These interactions allow the polymer chains of the hydrogel substrate to firmly adhere to the microgel nanoparticles through physical adsorption, generating molecular-level adhesion (Figure 2c-ii).¹⁴ Once adsorbed onto the substrate, the microgel particles become firmly fixed to the surface, and the probability of complete desorption of polymer chains decreases exponentially.^{41,42} The strength of this adhesion is determined by the type and quantity of noncovalent interactions between the substrate and the microgels.^{15,43} Therefore, at the molecular level, noncovalent interactions involving guanidinium cations are considered key factors in enhancing interfacial adhesion performance (Figure 2e).

At the mesoscopic scale, effective adhesion to the substrate surface is achieved by coating microgels onto the hydrogel matrix, which mimics the micronano structures found on the toe pads of natural organisms, thereby increasing the contact area and ensuring effective adhesion. Figure 2c-iv provides a

visual representation of this concept, using the gecko as a representative example.⁴⁴ As shown in Figure S9a, the adhesion interface of the original hydrogel substrate appears relatively smooth. In contrast, Figure S9b reveals that, in the absence of applied pressure, the interface of the hydrogel coated with microgel dispersions exhibits a microscopically heterogeneous morphology, where the initially continuous adhesion region is further segmented into multiple smaller contact areas by the microgel particles. According to the contact mechanics model, this phenomenon was found to enhance adhesion.⁴⁵ When microgels were applied to the hydrogel surface and covered with another hydrogel layer, deformation of the microgel became evident after 24 h of fixed-pressure treatment (Figure S10a,b). As shown in the adhesion cross-section in Figure S10c, this deformation caused the microgel particles to accumulate more distinctly and compactly into a blurred microgel layer at the hydrogel substrate interface, firmly anchoring the particles at specific positions on the interface. Specifically, the microgel particles are more densely arranged, leading to an increased contact area, significantly enhancing the interparticle interactions among microgel nanoparticles and thereby improving the cohesion of the microgel layer at the interface.⁴⁶ Furthermore, the deformation allowed the microgel to establish more extensive contact with the hydrogel substrate, increasing the interaction area and consequently amplifying the adhesion of the microgel. These results demonstrate that even in the absence of specific interaction groups, microgels can effectively enhance their adhesion by increasing the contact area (Figure 2e).

To further validate the proposed mechanism, MEO₂MA was incorporated into the microgels to confer temperature-responsive behavior. Consequently, the effect of temperature variation on adhesion performance was evaluated. As shown in Figure 3a, the adhesion of hydrogel coated with microgels decreases as the temperature increases, while the adhesion of the original hydrogel remains relatively constant (Figure S11). This indicates that the microgel dispersions can lead to a decrease in adhesion under temperature triggering, excluding the effects of other factors on adhesion. Since adhesion occurs at the interface, it is crucial to investigate the changes in the microgels at this interface. Figure 3b shows the dynamic light scattering (DLS) data for the temperature dependence of average hydrodynamic radius ($\langle R_h \rangle$) ("equivalent sphere radius" produced by an angular extrapolation of apparent diffusion coefficient of microgels) in ultrapure water, ranging from 25.0 to 65.0 °C. The data show a gradual decrease in $\langle R_h \rangle$ with increasing temperature, leveling off above 50.0 °C, and a swelling-to-deswelling transition at a volume phase transition temperature (VPTT) of approximately 42.8 °C. (as estimated from an asymmetric Lorentz fit of the first derivative of the $\langle R_h \rangle$).

At lower temperatures (<VPTT), the polymer networks are in a relatively swollen state relative to their state at the microgel synthesis temperature. On the molecular scale, guanidinium cations facilitate noncovalent interactions, enabling polymer chains to adsorb onto the surfaces of microgel particles. On the mesoscale, interactions between microgel particles enhance the cohesive strength of the interfacial microgel layer. Simultaneously, the microgels refine the pre-existing micro-adhesive regions of the hydrogel surface, significantly increasing the contact area at the interface, thereby providing effective adhesion. At higher temperatures (>VPTT), the hydrogen bonding between the microgel

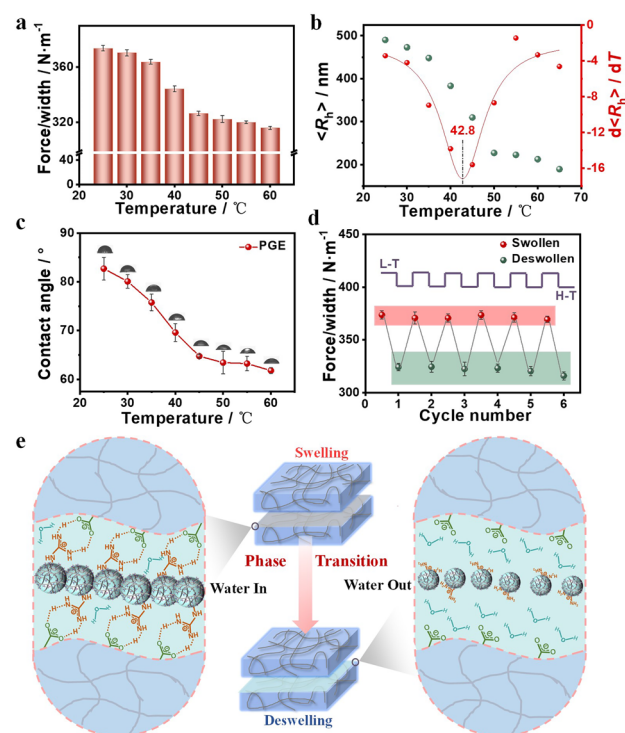


Figure 3. (a) T-peeling test of hydrogel substrates coated with microgel dispersions at different temperatures. (b) The $\langle R_h \rangle$ and first derivative with respect to temperature. The line is an asymmetric Lorentz fit. (c) The contact angle of deionized water droplets on hydrogel substrates coated with microgels at different temperatures. (d) Thermal-responsive reversible adhesion cycles of hydrogels coated with microgel adhesive in the swollen and deswollen states. (e) Tunable mechanisms of microgel dispersions. The data are expressed as means \pm standard deviations of triplicates.

network and surrounding water molecules is progressively disrupted, and free water migrates from the microgel matrix to the interface. This causes the microgels to shrink and their particle size to decrease. As shown in Figure S12, the significantly lower zeta potential of the microgel surface in the deswollen state compared to the swollen state indicates decreased freedom of the polymer chains,⁴⁷ along with the entrapment of a portion of the guanidinium groups within the microgel interior due to network collapse, limits their ability to interact effectively with the substrate. The accumulation of interfacial water triggers the reorganization of surface functional groups, with hydrophilic ether bond migrating outward and methoxy groups retreating toward the microgel interior as a result of phase-separation characteristics.⁴⁷ This mechanism was verified through in situ analysis of microgel dispersions coated on hydrogel substrates using the water droplet method. As shown in Figure 3c and Figure S13, the contact angle of the hydrogel substrate coated with the microgel dispersions decreased with increasing temperature, indicating a transition of the adhesive interface to a more hydrophilic state, and the interfacial wettability is enhanced. This result further demonstrates that the phase transition near the VPTT significantly increases the microscopic water content at the interface, excluding the possibility that temperature variations affect the contact angle of the native hydrogel substrate (Figure S14). The variation of functional groups on the microgel surface, driven by the accumulation of interfacial water, effectively shields the molecular interactions between the

polymer chains in the substrate and the microgel surface, ultimately leading to the desorption of polymer chains from the microgel surface. For the mesoscopic scale, the increased presence of water molecules on the microgel surface reduces particle–particle interactions, enhances lubrication, and lowers the cohesive strength of the microgel layer at the adhesive interface.⁴⁸ Additionally, the shrinkage of the microgels further decreases the contact area with the hydrogel substrate. These combined effects lead to a gradual reduction in the adhesion of the microgel adhesive as the temperature rises. Therefore, microgel dispersions regulate the adhesion performance of wet and soft materials by dynamically controlling interfacial water behavior under different swollen states and leveraging the synergistic contributions of molecular-scale and mesoscale factors, thereby providing effective adhesion.

Notably, when the temperature of the microgel dispersions falls below the volume phase transition temperature (VPTT), the interfacial adhesion is reactivated, exhibiting fully reproducible characteristics. As shown in Figure 3d, the adhesion of the microgel dispersions can be reversibly and repeatedly switched across six cycles through cyclic temperature control. During the second to sixth cycles, at lower temperatures, the microgels transition from a deswollen to a swollen state, reabsorbing interfacial free water and converting it into internal free water. The guanidine groups exposed on the microgel surface contribute to effective adhesion through the synergistic interactions of multiple factors at both molecular and mesoscopic scales. At higher temperatures, the microgels shrink, releasing internal free water to the interface, while some of the guanidine groups are encapsulated by the gel network, resulting in reduced adhesion. This further demonstrates that the regulation of microgel adhesion is a dynamic process, driven by the synergistic interaction of multiple factors across various scales (Figure 3e).

The effect of different swollen states of microgels on the adhesion properties of wet and soft materials was also investigated. Variations in the adhesion of microgel dispersions on different substrates were observed. In the swollen state, the microgel dispersions exhibited effective adhesion to various wet and soft materials, including different hydrogel substrates and pigskin (Figure 4a). The microgel particles formed a stable structure at the interface, effectively ensuring strong interfacial adhesion.⁴⁹ In the deswollen state, the adhesion of various substrates coated with microgel dispersions decreased (Figure 4b), a trend that was independent of the properties of the hydrogel itself (Figure S15). Figure 4c clearly illustrates that the microgel adhesive exhibits adhesion between two pieces of pigskin in its swollen state, while separating them in the deswollen state, further demonstrating the temperature tunability of the microgels. This tunability was also visually demonstrated through a Movie. The upper hydrogel layer was fixed to a rigid acrylic plate equipped with a smart temperature-controlled substrate, while the lower hydrogel layer was suspended by heavy weights.^{50,51} The weights themselves did not cause debonding (Movie S1). When the microgels transitioned from a swollen state to a deswollen state, the weights caused the hydrogel to peel forward until the two hydrogels are fully separated (Movie S2). The peeling cracks of the hydrogels exhibited different characteristics at various temperatures. Taking PHEMA as an example, in the swollen state, the hydrogel with the coated microgels showed rough notches upon tearing, and the two pieces of the hydrogel at the crack site were not fully separated, with irregular tear edges.

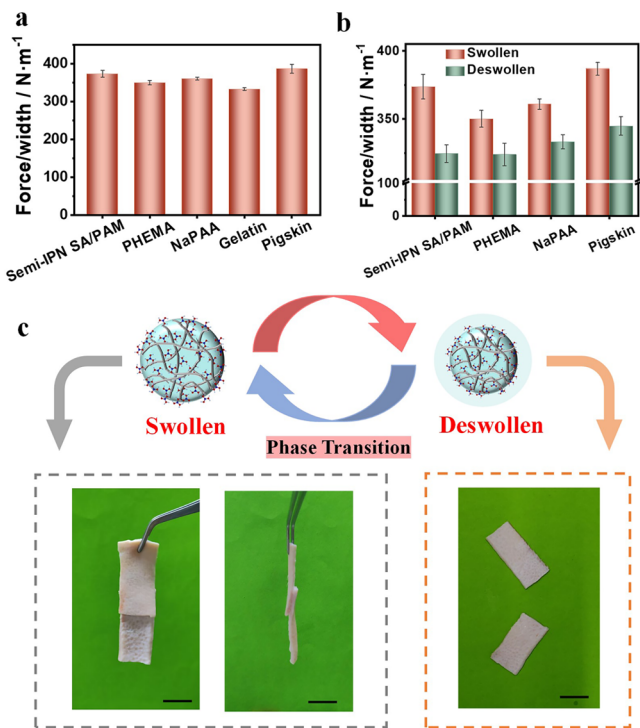


Figure 4. (a) T-peeling test of the microgel dispersions coated on different substrates in the swollen state. (b) T-peeling test of the microgel dispersions in different swollen state. The data are expressed as means \pm standard deviations of triplicates. (c) The images show the adhesion between two pieces of pigskin by the microgel dispersion in different states. (i) Front and (ii) side views of two pigskin pieces with adhesion by the microgel dispersions in the swollen state. (iii) Photos of two pigskin pieces separated in the deswollen state of the microgel dispersion. The scale bar is 2 cm.

This is consistent with the tearing behavior observed in two original hydrogels at 25.0 °C. However, in the deswollen state, the hydrogel with the coated microgels shows no notches upon tearing, and the two pieces of hydrogel are completely separated. At 50.0 °C, the tearing crack of the hydrogel without the coated microgels is similar to that in the swollen state. This further illustrates the temperature tunability of the microgel dispersions (Figure S16).

Experiments show that the hydrogel coated with microgel dispersions can firmly adhere to human skin and maintain strong adhesion under various bending and stretching motions of the fingers and arms. Even during dynamic movements, the adhesive's attachment to the skin remains intact and deforms with the skin's deformation, demonstrating that the microgel dispersions exhibit strong adaptability and can meet the needs of wearable devices subjected to dynamic changes (Figure S17). Carbon nanotubes were incorporated into the Semi-IPN SA/PAM hydrogel to make it electrically conductive.⁵² After installing electrodes on both sides of the hydrogel, it can be used as a strain sensor. By coating the hydrogel with microgel dispersions, it firmly adheres to the skin, and as the body stretches, the hydrogel's cross-sectional area changes, resulting in a variation in electrical resistance. When a voltage is applied, the hydrogel exhibits a linear change in resistance in response to body deformation, enabling the sensor to detect body movement with high sensitivity (Figure 5). As shown in Figures S18a–d, the microgel dispersion in its swollen state conformed to wrist movements without detachment. Upon

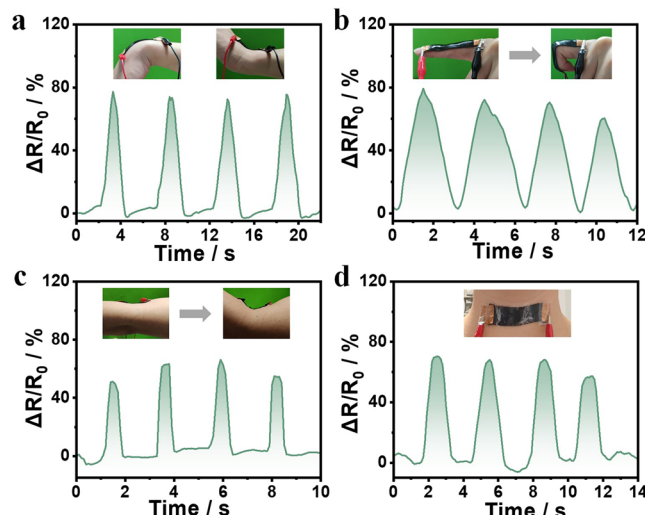


Figure 5. Human motion sensing. (a) Sensing of elbow bending. (b) Sensing of finger bending. (c) Sensing of arm bending. (d) Sensing of head tilting upward.

applying a hot bag to the hydrogel for 60 s, it detached from the skin. And the same phenomenon was observed during the eighth cycle, demonstrating that the microgel dispersion can be reused for at least eight cycles (Figures S18e–h). In addition, a comparative analysis of adhesion demonstrated that the microgel glue exhibited a markedly superior adhesive performance compared to other materials (Table S1).^{9,37,38,53–55} Therefore, the microgel dispersions have temperature-triggered adhesion and peeling properties, providing innovative design possibilities for the development of epidermal wearable devices.

In summary, we have developed a dynamic, multiscale, and multifactorial tunable adhesion strategy for wet and soft materials by harnessing phase transitions of the polymer network. Specifically, sprayable microgel nanoparticle glue regulate interfacial hydrodynamics, driven by their swelling and deswelling behavior. This allows for the reversible enhancement or reduction of adhesion by modifying the molecular interactions and contact area between the microgel particles and the substrate surface, as well as the cohesive forces within the interfacial microgel layer. Our study underscores the potential of polymer microgel dispersions as sprayable glues, as well as the phase transition in their inner polymer networks for dynamically controlling adhesion properties, thereby enabling their application in tunable adhesion of diverse wet and soft materials for advancing human-machine interface technologies.

■ ASSOCIATED CONTENT

SI Supporting Information

The Supporting Information is available free of charge at <https://pubs.acs.org/doi/10.1021/acsmacrolett.5c00169>.

Experimental details and supporting figures (PDF)

In the swollen state, the hydrogel retained adhesion (MP4)

In the deswollen state, the hydrogel detached on demand (MP4)

■ AUTHOR INFORMATION

Corresponding Author

Weitai Wu – State Key Laboratory for Physical Chemistry of Solid Surfaces, Collaborative Innovation Center of Chemistry for Energy Materials, The Key Laboratory for Chemical Biology of Fujian Province, and Department of Chemistry, College of Chemistry and Chemical Engineering, Xiamen University, Xiamen, Fujian 361005, China; orcid.org/0000-0003-3344-8883; Email: wwutxmu@xmu.edu.cn

Authors

Ting Zhao – State Key Laboratory for Physical Chemistry of Solid Surfaces, Collaborative Innovation Center of Chemistry for Energy Materials, The Key Laboratory for Chemical Biology of Fujian Province, and Department of Chemistry, College of Chemistry and Chemical Engineering, Xiamen University, Xiamen, Fujian 361005, China

Haojie Zhang – State Key Laboratory for Physical Chemistry of Solid Surfaces, Collaborative Innovation Center of Chemistry for Energy Materials, The Key Laboratory for Chemical Biology of Fujian Province, and Department of Chemistry, College of Chemistry and Chemical Engineering, Xiamen University, Xiamen, Fujian 361005, China

Jinmeng Zhang – State Key Laboratory for Physical Chemistry of Solid Surfaces, Collaborative Innovation Center of Chemistry for Energy Materials, The Key Laboratory for Chemical Biology of Fujian Province, and Department of Chemistry, College of Chemistry and Chemical Engineering, Xiamen University, Xiamen, Fujian 361005, China

Wen Chen – State Key Laboratory for Physical Chemistry of Solid Surfaces, Collaborative Innovation Center of Chemistry for Energy Materials, The Key Laboratory for Chemical Biology of Fujian Province, and Department of Chemistry, College of Chemistry and Chemical Engineering, Xiamen University, Xiamen, Fujian 361005, China

Jianda Xie – School of Materials Science and Engineering, Xiamen University of Technology, Xiamen, Fujian 361024, China

Complete contact information is available at:
<https://pubs.acs.org/10.1021/acsmacrolett.5c00169>

Author Contributions

T.Z. performed the experiment and wrote the manuscript. The rest of the authors participated in the design and discussion of the experiment and results. W.W. directed the whole program. The manuscript was written through contributions of all authors.

Notes

The authors declare no competing financial interest.

■ ACKNOWLEDGMENTS

This work is supported by National Natural Science Foundation of China (Nos. 21774105 and 20923004), Chuying Plan Youth Top-notch Talents of Fujian Province, Young and Middle-aged Teachers Education Scientific Research Project of Fujian Province (No. JAT200483), and National Fund for Fostering Talents of Basic Science (No. J1310024). We gratefully acknowledge Hengyu Shi (School of Economics, Xiamen University) for his valuable support in Statistical Analysis.

■ REFERENCES

- (1) Tee, B. C. K.; Chortos, A.; Berndt, A.; Nguyen, A. K.; Tom, A.; McGuire, A.; Lin, Z. C.; Tien, K.; Bae, W.-G.; Wang, H.; et al. A Skin-Inspired Organic Digital Mechanoreceptor. *Science* **2015**, *350*, 313–316.
- (2) Wirthl, D.; Pichler, R.; Drack, M.; Kettguber, G.; Moser, R.; Gerstmayr, R.; Hartmann, F.; Bradt, E.; Kaltseis, R.; Siket, C. M.; et al. Instant Tough Bonding of Hydrogels for Soft Machines and Electronics. *Sci. Adv.* **2017**, *3*, No. e1700053.
- (3) Liu, J.; Huang, Y. S.; Liu, Y.; Zhang, D.; Koynov, K.; Butt, H. J.; Wu, S. Reconfiguring Hydrogel Assemblies Using a Photocontrolled Metallocopolymer Adhesive for Multiple Customized Functions. *Nat. Chem.* **2024**, *16*, 1024–1033.
- (4) Yuk, H.; Varela, C. E.; Nabzdyk, C. S.; Mao, X.; Padera, R. F.; Roche, E. T.; Zhao, X. Dry Double-Sided Tape for Adhesion of Wet Tissues and Devices. *Nature* **2019**, *575*, 169–174.
- (5) Li, J.; Celiz, A. D.; Yang, J.; Yang, Q.; Wamala, I.; Whyte, W.; Seo, B. R.; Vasilyev, N. V.; Vlassak, J. J.; Suo, Z.; et al. Tough Adhesives for Diverse Wet Surfaces. *Science* **2017**, *357*, 378–381.
- (6) Cholewinski, A.; Yang, F.; Zhao, B. Algae-Mussel-Inspired Hydrogel Composite Glue for Underwater Bonding. *Mater. Horiz.* **2019**, *6*, 285–293.
- (7) Qin, C.; Ma, Y.; Zhang, Z.; Du, Y.; Duan, S.; Ma, S.; Pei, X.; Yu, B.; Cai, M.; He, X.; et al. Water-assisted Strong Underwater Adhesion Via Interfacial Water Removal and Self-adaptive Gelation. *Proc. Natl. Acad. Sci. U.S.A.* **2023**, *120*, No. e2301364120.
- (8) Tang, H.; Chen, Q.; Ke, X.; Wang, H.; Li, M.; Xie, J.; Luo, J.; Li, J. Bioinspired by Sandcastle Worm Glue: An Underwater Reversible Adhesive Modulated by pH Environments Based on Urushiol. *Ind. Eng. Chem. Res.* **2023**, *62*, 19690–19701.
- (9) Zheng, Y.; Wu, M.; Duan, M.; Jin, Q.; Chen, S.; Wang, X.; Zhou, D. Skin Temperature-Triggered Switchable Adhesive Coatings for Wearing Comfortable Epidermal Electronics. *Chem. Eng. J.* **2024**, *488*, No. 150459.
- (10) Zhao, Y. H.; Wu, Y.; Wang, L.; Zhang, M. M.; Chen, X.; Liu, M. J.; Fan, J.; Liu, J. Q.; Zhou, F.; Wang, Z. K. Bio-inspired reversible underwater adhesive. *Nat. Commun.* **2017**, *8*, 2218.
- (11) Zheng, S. Y.; Zhou, J.; Wang, S.; Wang, Y. J.; Liu, S.; Du, G.; Zhang, D.; Fu, J.; Lin, J.; Wu, Z. L.; Zheng, Q.; Yang, J. T. Water-Triggered Spontaneously Solidified Adhesive: From Instant and Strong Underwater Adhesion to In Situ Signal Transmission. *Adv. Funct. Mater.* **2022**, *32*, No. 2205597.
- (12) Fan, H. L.; Gong, J. P. Bioinspired Underwater Adhesives. *Adv. Mater.* **2021**, *33*, No. 2102983.
- (13) Zhang, Z.; Qin, C.; Feng, H.; Xiang, Y.; Yu, B.; Pei, X.; Ma, Y.; Zhou, F. Design of Large-Span Stick-Slip Freely Switchable Hydrogels Via Dynamic Multiscale Contact Synergy. *Nat. Commun.* **2022**, *13*, 6964.
- (14) Rose, S.; Prevoteau, A.; Elzière, P.; Hourdet, D.; Marcellan, A.; Leibler, L. Nanoparticle Solutions as Adhesives for Gels and Biological Tissues. *Nature* **2014**, *505*, 382–385.
- (15) Hao, L. T.; Park, S.; Choy, S.; Kim, Y.-M.; Lee, S.-W.; Ok, Y. S.; Koo, J. M.; Hwang, S. Y.; Hwang, D. S.; Park, J.; et al. Strong, Multifaceted Guanidinium-Based Adhesion of Bioorganic Nanoparticles to Wet Biological Tissue. *JACS Au* **2021**, *1*, 1399–1411.
- (16) Liu, Y.; Li, Y.; Tan, J.; Cheng, P.; Yang, M.; Li, B.; Wang, Q.; Mequanint, K.; Zhu, C.; Xing, M.; et al. Gelation of Highly Entangled Hydrophobic Macromolecular Fluid for Ultrastrong Underwater in Situ Fast Tissue Adhesion. *Sci. Adv.* **2022**, *8*, No. eabm9744.
- (17) Shi, Z.; Wang, Z.; Xiao, K.; Zhu, B.; Wang, Y.; Zhang, X.; Lin, Z.; Tan, D.; Xue, L. Bioinspired Touch-Responsive Hydrogels for On-Demand Adhesion on Rough Surfaces. *ACS Appl. Mater. Interfaces* **2024**, *16*, 19819–19827.
- (18) Bae, W. G.; Kim, H. N.; Kim, D.; Park, S. H.; Jeong, H. E.; Suh, K. Y. 25th Anniversary Article: Scalable Multiscale Patterned Structures Inspired by Nature: The Role of Hierarchy. *Adv. Mater.* **2014**, *26*, 675–700.
- (19) Autumn, K.; Liang, Y. A.; Hsieh, S. T.; Zesch, W.; Chan, W. P.; Kenny, T. W.; Fearing, R.; Full, R. J. Adhesive Force of a Single Gecko Foot-Hair. *Nature* **2000**, *405*, 681–685.
- (20) Matter, M. T.; Starsich, F.; Galli, M.; Hilber, M.; Schlegel, A. A.; Bertazzo, S.; Pratsinis, S. E.; Herrmann, I. K. Developing a Tissue Glue by Engineering the Adhesive and Hemostatic Properties of Metal Oxide Nanoparticles. *Nanoscale* **2017**, *9*, 8418–8426.
- (21) Pan, Z.; Fu, Q.-Q.; Wang, M.-H.; Gao, H.-L.; Dong, L.; Zhou, P.; Cheng, D.-D.; Chen, Y.; Zou, D.-H.; He, J.-C.; et al. Designing Nanohesives for Rapid, Universal, and Robust Hydrogel Adhesion. *Nat. Commun.* **2023**, *14*, 5378.
- (22) Arno, M. C.; Inam, M.; Weems, A. C.; Li, Z.; Binch, A. L. A.; Platt, C. I.; Richardson, S. M.; Hoyland, J. A.; Dove, A. P.; O'Reilly, R. K. Exploiting the Role of Nanoparticle Shape in Enhancing Hydrogel Adhesive and Mechanical Properties. *Nat. Commun.* **2020**, *11*, 1420.
- (23) Appel, E. A.; Tibbitt, M. W.; Webber, M. J.; Mattix, B. A.; Veiseh, O.; Langer, R. Self-Assembled Hydrogels Utilizing Polymer-Nanoparticle Interactions. *Nat. Commun.* **2015**, *6*, 6295.
- (24) Cao, Z.; Dobrynin, A. V. Nanoparticles as Adhesives for Soft Polymeric Materials. *Macromolecules* **2016**, *49*, 3586–3592.
- (25) Xie, K.; Gao, X.; Xiao, C.; Molinari, N.; Angioletti-Uberti, S. Rationalizing the Effect of Shape and Size in Nanoparticle-Based Glues. *J. Phys. Chem. C* **2022**, *126*, 7517–7528.
- (26) Kim, J.-H.; Kim, H.; Choi, Y.; Lee, D. S.; Kim, J.; Yi, G.-R. Colloidal Mesoporous Silica Nanoparticles as Strong Adhesives for Hydrogels and Biological Tissues. *ACS Appl. Mater. Interfaces* **2017**, *9*, 31469–31477.
- (27) Karg, M.; Pich, A.; Hellweg, T.; Hoare, T.; Lyon, L. A.; Crassous, J. J.; Suzuki, D.; Gumerov, R. A.; Schneider, S.; Potemkin, I. I.; et al. Nanogels and Microgels: From Model Colloids to Applications, Recent Developments, and Future Trends. *Langmuir* **2019**, *35*, 6231–6255.
- (28) Keidel, R.; Ghavami, A.; Lugo, D. M.; Lotze, G.; Virtanen, O.; Beumers, P.; Pedersen, J. S.; Bardow, A.; Winkler, R. G.; Richtering, W. Time-Resolved Structural Evolution During the Collapse of Responsive Hydrogels: The microgel-to-particle transition. *Sci. Adv.* **2018**, *4*, No. aaaa07086.
- (29) Del Monte, G.; Truzzolillo, D.; Camerin, F.; Ninarello, A.; Chauveau, E.; Tavagnacco, L.; Gnan, N.; Rovigatti, L.; Sennato, S.; Zaccarelli, E. Two-Step Deswelling in the Volume Phase Transition of Thermoresponsive Microgels. *Proc. Natl. Acad. Sci. U.S.A.* **2021**, *118*, No. 2109560118.
- (30) Shen, C.; Cheng, Y.; Peng, Z.; Chen, S. Switchable Adhesion of Gecko-Inspired Hierarchically Wedge-Mushroom-Shaped Surface. *Chem. Eng. J.* **2024**, *488*, No. 150900.
- (31) Lutz, J.-F.; Hoth, A. Preparation of Ideal PEG Analogues with a Tunable Thermosensitivity by Controlled Radical Copolymerization of 2-(2-Methoxyethoxy)ethyl Methacrylate and Oligo(ethylene glycol) Methacrylate. *Macromolecules* **2006**, *39*, 893–896.
- (32) Medeiros, S. F.; Oliveira, P. F. M.; Silva, T. M.; Lara, B. R.; Elaissari, A.; Santos, A. M. Biocompatible and multi-responsive poly(N-vinylcaprolactam)-based microgels: The role of acidic comonomers in the colloidal properties and phase transition as a function of temperature and pH. *Eur. Polym. J.* **2015**, *73*, 191–201.
- (33) Jones, C. D.; Lyon, L. A. Synthesis and Characterization of Multiresponsive Core-Shell Microgels. *Macromolecules* **2000**, *33*, 8301–8306.
- (34) Wang, X.; Qiu, H.; Wu, Q.; Xie, J.; Zhou, S.; Wu, W. Salt-Enhanced CO₂-Responsiveness of Microgels. *ACS Macro Lett.* **2020**, *9*, 1611–1616.
- (35) Wieczorek, W.; Raducha, D.; Zalewska, A.; Stevens, J. R. Effect of Salt Concentration on the Conductivity of PEO-Based Composite Polymeric Electrolytes. *J. Phys. Chem. B* **1998**, *102*, 8725–8731.
- (36) Kalaiselvi, D.; Kumar, R. M.; Jayavel, R. Single Crystal Growth and Properties of Semiorganic Nonlinear Optical L-Arginine Hydrochloride Monohydrate Crystals. *Crist. Res. Technol.* **2008**, *43*, 851–856.
- (37) Yang, J.; Bai, R.; Suo, Z. Topological Adhesion of Wet Materials. *Adv. Mater.* **2018**, *30*, No. e1800671.

- (38) Zhang, J. N.; Zhu, H. W.; Liu, T. Q.; Chen, Y. Y.; Jiao, C.; He, C. C.; Wang, H. L. Strong Adhesion of Hydrogels by Polyelectrolyte Adhesives. *Polymer* **2020**, *206*, No. 122845.
- (39) Zhang, J.; Wang, W.; Zhang, Y.; Wei, Q.; Han, F.; Dong, S.; Liu, D.; Zhang, S. Small-Molecule Ionic Liquid-Based Adhesive with Strong Room-Temperature Adhesion Promoted by Electrostatic Interaction. *Nat. Commun.* **2022**, *13*, 5214.
- (40) Heyda, J.; Okur, H. I.; Hladíková, J.; Rembert, K. B.; Hunn, W.; Yang, T.; Dzubiella, J.; Jungwirth, P.; Cremer, P. S. Guanidinium can both Cause and Prevent the Hydrophobic Collapse of Biomacromolecules. *J. Am. Chem. Soc.* **2017**, *139*, 863–870.
- (41) Netz, R. R.; Andelman, D. Neutral and Charged Polymers at Interfaces. *Phys. Rep.* **2003**, *380*, 1–95.
- (42) Santore, M. M. Dynamics in Adsorbed Homopolymer Layers: Understanding Complexity from Simple Starting Points. *Curr. Opin. Colloid In.* **2005**, *10*, 176–183.
- (43) Gao, H.; Wang, X.; Yao, H.; Gorb, S.; Arzt, E. Mechanics of Hierarchical Adhesion Structures of Geckos. *Mech. Mater.* **2005**, *37*, 275–285.
- (44) Autumn, K.; Niewiarowski, P. H.; Puthoff, J. B. Gecko Adhesion as a Model System for Integrative Biology, Interdisciplinary Science, and Bioinspired Engineering. *Annu. Rev. Ecol. Evol. Syst.* **2014**, *45*, 445–470.
- (45) Arzt, E.; Gorb, S.; Spolenak, R. From Micro to Nano Contacts in Biological Attachment Devices. *Proc. Natl. Acad. Sci. U.S.A.* **2003**, *100*, 10603–10606.
- (46) Spears, M. W.; Herman, E. S.; Gaulding, J. C.; Lyon, L. A. Dynamic Materials from Microgel Multilayers. *Langmuir* **2014**, *30*, 6314–6323.
- (47) Rodríguez-Díaz, F.; Castellanos-Suárez, A.; Lozsán, A. A Phenomenological Order Approach to the Volume Phase Transition in Microgel Particles. *Phys. Chem. Chem. Phys.* **2017**, *19*, 16541–16554.
- (48) He, B.; Chen, L.; Biehl, P.; Meng, X.; Chen, W.; Xu, D.; Ren, J.; Zhang, K. Scale-Spanning Strong Adhesion Using Cellulose-Based Microgels. *Small* **2023**, *19*, No. 2300865.
- (49) Meddahi-Pelle, A.; Legrand, A.; Marcellan, A.; Louedec, L.; Letourneur, D.; Leibler, L. Organ Repair, Hemostasis, and in Vivo Bonding of Medical Devices by Aqueous Solutions of Nanoparticles. *Angew. Chem., Int. Ed.* **2014**, *53*, 6369–6373.
- (50) Sugizaki, Y.; Shiina, T.; Tanaka, Y.; Suzuki, A. Effects of peel angle on peel force of adhesive tape from soft adherend. *J. Adhes. Sci. Technol.* **2016**, *30*, 2637–2654.
- (51) Liu, J.; Yang, C.; Yin, T.; Wang, Z.; Qu, S.; Suo, Z. Polyacrylamide hydrogels. II. elastic dissipater. *J. Mech. Phys. Solids* **2019**, *133*, No. 103737.
- (52) Khan, M.; Shah, L. A.; Rahman, T. U.; Ara, L.; Yoo, H. M. Multiple-Language-Responsive Conductive Hydrogel Composites for Flexible Strain and Epidermis Sensors. *ACS Appl. Polym. Mater.* **2024**, *6*, 4233–4243.
- (53) Zhang, Y.; Dai, Y.; Xia, F.; Zhang, X. Gelatin/polyacrylamide ionic conductive hydrogel with skin temperature-triggered adhesion for human motion sensing and body heat harvesting. *Nano Energy* **2022**, *104*, No. 107977.
- (54) Zhang, Y.; Li, C.; Guo, A.; Yang, Y.; Nie, Y.; Liao, J.; Liu, B.; Zhou, Y.; Li, L.; Chen, Z.; et al. Black phosphorus boosts wet-tissue adhesion of composite patches by enhancing water absorption and mechanical properties. *Nat. Commun.* **2024**, *15*, 1618.
- (55) Qiu, J.; Ma, H.; Yao, M.; Song, M.; Zhang, L.; Xu, J.; Liu, X.; Lu, B. Design of a supersoft, ultra-stretchable, and 3D printable hydrogel electrical bioadhesive interface for electromyography monitoring. *Supramol. Mater.* **2024**, *3*, No. 100079.